Published OnlineFirst on September 7, 2010 as 10.1158/0008-5472.CAN-10-0766

Cancer Research

Discovery and Canine Preclinical Assessment of a Nontoxic Procaspase-3–Activating Compound

Quinn P. Peterson[1], Danny C. Hsu[2], Chris J. Novotny[1], Diana C. West[2], Dewey Kim[2], Joanna M. Schmit[4], Levent Dirikolu[3], Paul J. Hergenrother[1,2], and Timothy M. Fan[4]

Abstract

A critical event in the apoptotic cascade is the proteolytic activation of procaspases to active caspases. The caspase autoactivating compound PAC-1 induces cancer cell apoptosis and exhibits antitumor activity in murine xenograft models when administered orally as a lipid-based formulation or implanted s.c. as a cholesterol pellet. However, high doses of PAC-1 were found to induce neurotoxicity, prompting us to design and assess a novel PAC-1 derivative called S-PAC-1. Similar to PAC-1, S-PAC-1 activated procaspase-3 and induced cancer cell apoptosis. However, S-PAC-1 did not induce neurotoxicity in mice or dogs. Continuous i.v. infusion of S-PAC-1 in dogs led to a steady-state plasma concentration of ~10 μmol/L for 24 to 72 hours. In a small efficacy trial of S-PAC-1, evaluation of six pet dogs with lymphoma revealed that S-PAC-1 was well tolerated and that the treatments induced partial tumor regression or stable disease in four of six subjects. Our results support this canine setting for further evaluation of small-molecule procaspase-3 activators, including S-PAC-1, a compound that is an excellent candidate for further clinical evaluation as a novel cancer chemotherapeutic. *Cancer Res; 70(18); 7232–41. ©2010 AACR.*

Introduction

Members of the caspase family of cysteine proteases are key players in both the initiation and execution of apoptosis. These enzymes exist in the cell as low-activity zymogens (proenzymes) that are proteolytically activated to the mature, highly active enzyme. Most critical to apoptosis is the proteolytic conversion of procaspase-3 to caspase-3. As both the intrinsic and extrinsic apoptotic pathways converge to activate procaspase-3, and as caspase-3 has >100 cellular substrates, the activation of procaspase-3 to caspase-3 is a pivotal and committed event in the apoptotic cascade. Interestingly, procaspase-3 is overexpressed in a variety of tumor histologies, including breast cancer (1), colon cancer (2), lung cancer (3), lymphoma (4), neuroblastoma (5), melanoma (6), and liver cancer (7), suggesting that a small molecule that activates procaspase-3 could have selectivity for cancer cells versus normal cells.

In 2006, we reported the discovery of a small molecule, called PAC-1 (Fig. 1A), which enhances procaspase-3 activity *in vitro*, induces death in cancer cells in culture, and has efficacy in multiple mouse xenograft models when administered orally as a lipid-based formulation or implanted s.c. as a cholesterol pellet (8). PAC-1 activates procaspase-3 *in vitro* through the chelation of inhibitory zinc ions (9), and derivative synthesis and evaluation reveal that the biological activity of PAC-1 is tied to having an intact *ortho*-hydroxy *N*-acyl hydrazone zinc-chelating motif (10). Evidence suggests that PAC-1 induces apoptotic death in cancer cells through the chelation of zinc from procaspase-3, most notably the colocalization of a fluorescent PAC-1 derivative with sites of cellular caspase-3 activity (10).

As the first procaspase-activating compound, experiments with PAC-1 can begin to define the potential of procaspase-3 activation as a viable anticancer strategy. To further develop PAC-1 as an experimental therapeutic for the treatment of cancer in humans, we sought to characterize the effect of this compound when administered i.v. and in more sophisticated *in vivo* tumor model systems, specifically canines with spontaneous cancer. The evaluation of experimental therapeutics in pet dogs with cancer offers many advantages over murine xenograft models (11). Herein, we report toxicity studies of i.v. administered PAC-1 in mice, and the discovery of a novel PAC-1 derivative (called S-PAC-1) that induces apoptosis in cancer cell lines in culture, is well-tolerated in mice and research dogs, and has moderate activity in a small trial of canine patients with spontaneous lymphoma. These results show the feasibility of S-PAC-1 administration to pet dogs with lymphoma as a means to evaluate the therapeutic potential of this class of compounds.

Authors' Affiliations: Departments of [1]Biochemistry, [2]Chemistry, [3]Veterinary Biosciences, and [4]Veterinary Clinical Medicine, University of Illinois, Urbana, Illinois

Note: Supplementary data for this article are available at Cancer Research Online (http://cancerres.aacrjournals.org/).

Corresponding Authors: Paul J. Hergenrother, University of Illinois, 600 South Mathews, Urbana, IL 61801. Phone: 217-333-0363; Fax: 217-244-8024; E-mail: hergenro@illinois.edu or Timothy M. Fan, University of Illinois, 1008 West Hazelwood Drive, Urbana, IL 61801. Phone: 217-333-5300; E-mail: t-fan@illnois.edu.

doi: 10.1158/0008-5472.CAN-10-0766

Materials and Methods

Cell lines and reagents

U-937, Jurkat, SK-MEL-5, HeLa, MDA-MB-231, and EL4 cells were obtained from the American Type Culture Collection (authenticated by short tandem repeat analysis) and maintained at low passage number. Two canine B-cell lymphoma lines (17-71 and GL-1) were provided by Dr. Steve Suter (North Carolina State University, Raleigh, NC). All cultures were maintained in RPMI 1640 supplemented with 10% fetal bovine serum and 1% penicillin-streptomycin and grown at 37°C and 5% CO_2. PAC-1 was synthesized as previously described (8). S-PAC-1 was synthesized as described in the Supplementary Data. Ac-DEVD-pNA was synthesized as previously described (12). Chelex-treated HEPES-NaCl buffer is 50 mmol/L HEPES and 300 mmol/L NaCl and is treated with Chelex resin for 1 hour before use.

EGTA fluorescence titration assay

EGTA fluorescence titration assay was performed according to a developed protocol (13) exactly as previously reported (10).

Recombinant expression, purification, and evaluation of uncleavable procaspase-3 mutant (D_3A)

Procaspase-3 D_3A was expressed and purified exactly as previously reported (10).

Procaspase-3 activation

Recombinantly expressed, zinc-free procaspase-3 D_3A (7.5 μmol/L) in Chelex-treated HEPES-NaCl was incubated in the presence of $ZnSO_4$ (10 μmol/L), and the basal activity was assessed by addition of Ac-DEVD-pNA substrate (200 μmol/L) and monitored at 405 nm with a SpectraMax plate reader (Molecular Devices). After the basal activity was determined, DMSO, PAC-1, or S-PAC-1 was added to each sample to a final concentration of 50 μmol/L. Activity of each stock was assessed as described above every 20 minutes. The slope of each data set was used to determine the activity of the protein. Protein activity was normalized to a percent activity at each time point using a zinc-free sample as 100% activity and the DMSO control as 0% activity controls.

Apoptosis and cytotoxicity assays

Induction of apoptosis was assessed exactly as previously reported (10). Cell death IC_{50} values were assessed by sulforhodamine B assay exactly as previously reported (10) or by MTS assay (Promega) according to the manufacturer's suggested protocol.

Toxicity determinations of PAC-1 and S-PAC-1

PAC-1 and S-PAC-1 were formulated in 2-hydroxypropyl-β-cyclodextrin (HPβCD; ref. 14) as described in the Supplementary Data. C57/BL6 mice were administered varying doses of either PAC-1 or S-PAC-1 via tail vein injection. Mice were monitored by observation for a period of 24 hours for signs of toxicity, including sensitivity to touch, hypothermia, hunched posture, agitation, and rapid or depressed breathing.

Pharmacokinetics of S-PAC-1 in healthy research dogs and dogs with lymphoma

Four healthy male hound dogs weighing at least 30 kg were used for all preclinical pharmacokinetic studies. All dogs received a single dose of S-PAC-1 via i.v. injection. After a 2-week washout period, three dogs received a dosing regimen predicted to achieve and maintain a steady-state plasma concentration of 10 μmol/L, that is, i.v. S-PAC-1 delivered as a constant-rate infusion comprising a 10-minute loading dose, followed by a constant maintenance dose for 24 hours. Dogs with lymphoma were treated with i.v. S-PAC-1 in a constant-rate infusion for either 24 or 72 hours. For all dogs and dosing strategies, blood was drawn from the lateral saphenous vein and centrifuged, and plasma was stored at −80°C until analysis.

Toxicologic assessment of S-PAC-1 in healthy research dogs

Toxicity of S-PAC-1 administration was determined by serial weekly complete blood counts, serum biochemistry panels, and animal caregiver gastrointestinal toxicity observational scores adhering to the Veterinary Co-operative Oncology Group Common Terminology Criteria for Adverse Events (VCOG-CTCAE).

Antitumor assessment of S-PAC-1 in dogs with lymphoma

Caliper measurement was performed according to the Response Evaluation Criteria in Solid Tumors (RECIST) method (15). Briefly, the longest linear length measurement was recorded for four pairs of peripheral lymph nodes (mandibular, prescapular, inguinal, and popliteal), with the summation of these values giving a RECIST score. In addition to caliper measurements for all four sets of peripheral lymph nodes, computed tomography (CT) scans were performed on the mandibular lymph nodes in every patient, allowing for accurate and objective measurement of maximal lymph node linear length.

Results

In vivo toxicity of PAC-1

In an effort to characterize the feasibility and tolerability of i.v. administered PAC-1, toxicity testing of PAC-1 (when administered in HPβCD via tail vein injection) was carried out with C57/BL6 mice and is summarized in Supplementary Table S1. Mice that received PAC-1 exhibited transient neurotoxicity with onset occurring within 5 minutes of drug administration and resolution occurring within 2 hours. Mice that received only the HPβCD vehicle did not exhibit any clinically observable toxicity. The observed neurotoxicity of PAC-1 in mice did not seem to be species specific, as grand mal seizure activity in one healthy dog was elicited when administered 25 mg/kg of PAC-1 as a 5-minute i.v.

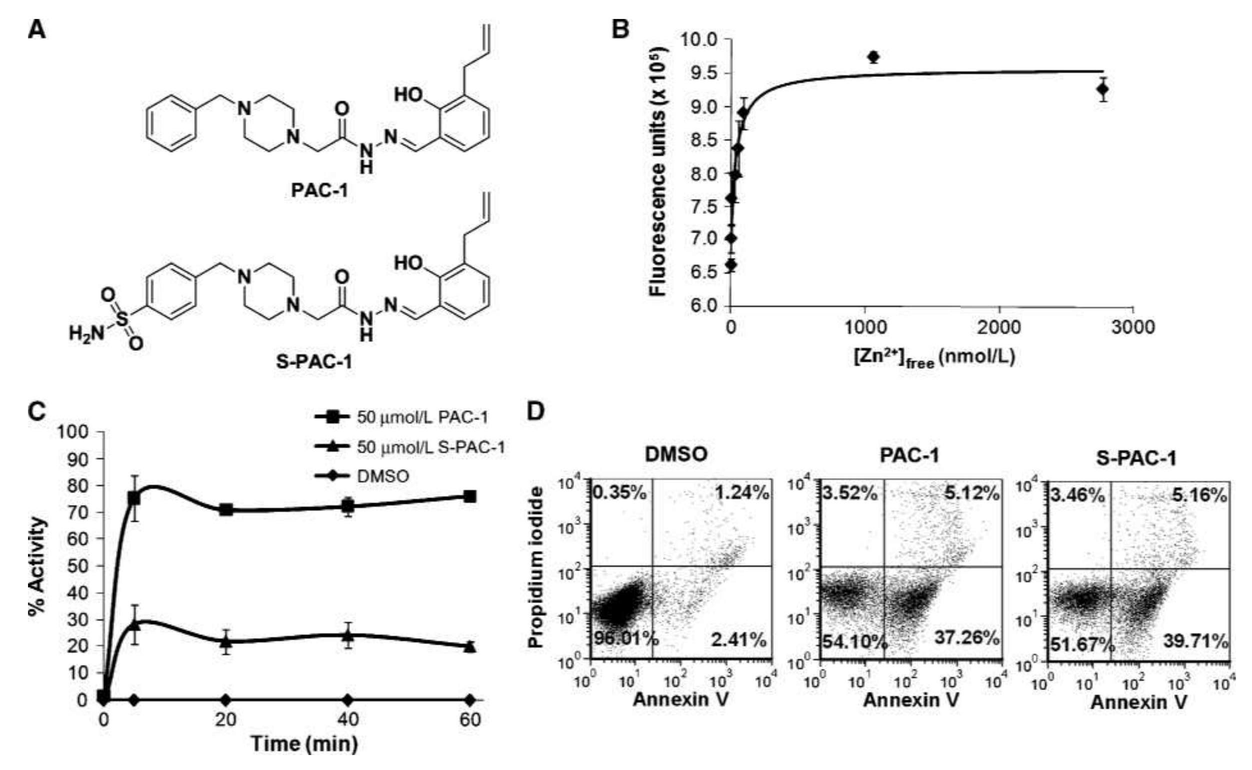

Figure 1. *In vitro* assessment of PAC-1 and S-PAC-1. A, structures of PAC-1 and S-PAC-1. B, the formation curve of the Zn^{2+}–S-PAC-1 complex as determined by EGTA titration. S-PAC-1 binds zinc with a K_d of 46 ± 5 nmol/L. Points, mean (n = 3); bars, SE. C, PAC-1 and S-PAC-1 induce rapid relief of zinc-mediated inhibition of procaspase-3 (D_3A). Using a chromogenic Ac-DEVD-pNA substrate, the activity of procaspase-3 (7.5 μmol/L) was assessed in the presence of inhibitory zinc (10 μmol/L) and vehicle, PAC-1, or S-PAC-1 (50 μmol/L). Maximal activity is observed after a 5-min incubation with compound. Points, mean (n = 3); bars, SE. D, PAC-1 and S-PAC-1 both induce apoptotic cell death in U-937 cells as shown by a population of Annexin V–positive, PI-negative cells. Data are representative of three separate experiments.

infusion. Adverse side effects in this dog were transient and not life limiting.

Given the known affinity of PAC-1 for zinc *in vitro* (9), and the data suggesting that PAC-1 binds cellular zinc (10), we hypothesized that the neurotoxicity observed in mice and dogs administered PAC-1 in HPβCD was caused by the chelation of intracellular zinc at *N*-methyl-D-aspartic acid (NMDA) receptors within the central nervous system (CNS). This hypothesis is consistent with data from *in vivo* studies of other zinc chelators that induce a neurologic phenotype reminiscent of what we observed with PAC-1 (16, 17). Indeed, *in silico* analysis of PAC-1 to predict the partitioning across the blood-brain barrier (BBB; ref. 18) shows that PAC-1 has a calculated logBB of −0.07. This logBB would correlate to a partitioning ratio of 1.0:0.85 between the blood and the brain, suggesting that a significant amount of PAC-1 may be entering the CNS. Several studies have indicated that chelation of intracellular zinc stores relieves tonic suppression of NMDA receptors, resulting in neuronal hyperexcitation (17, 19).

Design of S-PAC-1

In an effort to overcome the undesirable side effect of neurotoxicity, we hypothesized that a derivative of PAC-1 that had a lower propensity to cross the BBB would exhibit decreased neurotoxicity and allow for dosing at higher concentrations. Based on the structure-activity relationship previously reported (10), it was predicted that a polar functional group installed on the benzyl ring of PAC-1 should decrease the predicted logBB while maintaining the activity of the parent compound. As such S-PAC-1 (Fig. 1A), a sulfonamide derivative of PAC-1, was designed as a compound predicted to have a markedly decreased ability to cross the BBB (logBB of −1.26, providing a predicted blood/brain ratio of 1.0:0.055). See Supplementary Data for the synthetic route to S-PAC-1.

S-PAC-1 binds zinc *in vitro*

The activity of S-PAC-1 was characterized in several biochemical assays analogous to previously performed PAC-1 studies (9, 10). An EGTA competition titration experiment (13) was used to determine the binding constant for the S-PAC-1–Zn^{2+} complex. In the presence of EGTA, the changes in the fluorescence of the S-PAC-1–Zn^{2+} complex were used to plot a formation curve (Fig. 1B). Using the known binding constant of EGTA, the free zinc concentration can be calculated and used to determine the binding constant of the

S-PAC-1–Zn^{2+} complex. This complex has a K_d of 46 ± 5 nmol/L compared with 52 ± 2 nmol/L for PAC-1–Zn^{2+} (10).

S-PAC-1 activates procaspase-3 *in vitro*

The ability of S-PAC-1 to activate recombinantly expressed procaspase-3 in the presence of exogenous zinc was assessed *in vitro*. To ensure that the enzymatic activity of the proenzyme was being monitored, a proteolytically uncleavable mutant of procaspase-3 was used in which the three aspartic acid cleavage site residues are mutated to alanine (D9A/D28A/D175A; refs. 9, 20). This uncleavable form of procaspase-3 is not capable of processing to the mature active caspase-3, thus ensuring that any increase in activity observed is due to an increase in the activity of the proenzyme rather than autoproteolysis of the proenzyme. As shown in Fig. 1C, S-PAC-1 rapidly (within 5 minutes) enhances the enzymatic activity of the proenzyme by relief of zinc-mediated inhibition, although to a lesser degree than PAC-1.

S-PAC-1 induces death in multiple cancer cell lines in culture

Having confirmed that S-PAC-1 chelates zinc and activates procaspase-3 *in vitro*, the antineoplastic activity of S-PAC-1 was assessed against a panel of human, canine, and murine cancer cell lines using the sulforhodamine B assay (21). The 72-hour IC_{50} values for PAC-1 and S-PAC-1 are reported in Table 1. Both PAC-1 and S-PAC-1 have micromolar cytotoxic IC_{50} values against all lymphoma cell lines tested regardless of the species of origin. U-937 cells treated with DMSO, 50 μmol/L PAC-1, or 50 μmol/L S-PAC-1 for 12 hours were assessed by Annexin V/propidium iodide (PI) staining and analyzed by flow cytometry (Fig. 1D). Both PAC-1 and S-PAC-1 treatment lead to a similar increase in the population of apoptotic cells (Annexin V positive, PI negative).

In an effort to determine an appropriate treatment strategy for the evaluation of S-PAC-1 *in vivo*, the time dependency of S-PAC-1 cytotoxicity was evaluated. U-937 cells were treated with S-PAC-1 for various lengths of time. After treatment with S-PAC-1, cells were washed to remove compound and cultured in growth medium without compound. Cell death was assessed at 72 hours for all treatment times. An IC_{50} value was determined for each exposure time and reported in Table 1. At times shorter than 6 hours, the IC_{50} value was greater than the highest concentration tested. Between 12 and 24 hours, the IC_{50} value rapidly decreased to a minimum and showed little variation over the course of the subsequent 48 hours. These time dependency experiments suggest that S-PAC-1 will be most effective *in vivo* if cancer cells are exposed to the compound for at least 24 hours.

S-PAC-1 has no detectable neurotoxic effect in mice

Having confirmed the activity of S-PAC-1 *in vitro* and in cell culture, the toxicity of S-PAC-1 (when administered in HPβCD via tail vein injection) was assessed in C57/BL6 mice and is summarized in Supplementary Table S1. S-PAC-1 exhibited no observable toxicity at any dose tested. Given the dramatically reduced neurotoxic effect of S-PAC-1, pharmacokinetic analysis was performed to compare the plasma concentrations achievable with PAC-1 and S-PAC-1. Mice were treated with 20 mg/kg PAC-1 (the dose at which significant neurologic symptoms first appear), 50 mg/kg PAC-1 (the dose where acute neurologic symptoms are present),

Table 1. Assessment of PAC-1 and S-PAC-1 cytotoxicity in cancer cell lines

Cell line	Species	Origin	Exposure time (h)	S-PAC-1 72-h IC_{50} (μmol/L)	PAC-1 72-h IC_{50} (μmol/L)
U-937	Human	Lymphoma	1	>100	—
			3	>100	—
			6	>100	—
			9	20 ± 12	—
			12	9.7 ± 1.1	—
			24	5.9 ± 1.0	—
			48	5.6 ± 0.8	—
			72	6.4 ± 0.8	9.3 ± 0.5
EL4	Mouse	Lymphoma	72	7.1 ± 1.3	3.8 ± 0.9
17-71*	Dog	Lymphoma	72	2.7 ± 0.8	2.5 ± 0.9
GL-1	Dog	Lymphoma	72	7.1 ± 0.3	4.9 ± 0.3
OSW	Dog	Lymphoma	72	11.0 ± 0.9	8.6 ± 1.3
Jurkat	Human	Leukemia	72	4.5 ± 1.1	5.7 ± 2.8
SK-MEL-5	Human	Melanoma	72	8.6 ± 1.3	11.5 ± 3.6
HeLa	Human	Cervical	72	28.4 ± 7.7	15.5 ± 3.8
MDA-MB-231	Human	Breast	72	11.7 ± 5.3	9.9 ± 1.0

NOTE: Error is SEM (n = 3). Cells were exposed to compound for the time indicated, compound was washed out, and cell viability/biomass assessment was made after 72 h.

*This cell line was assessed using the MTS cell viability assay. All other cell lines were assessed with the sulforhodamine B assay.

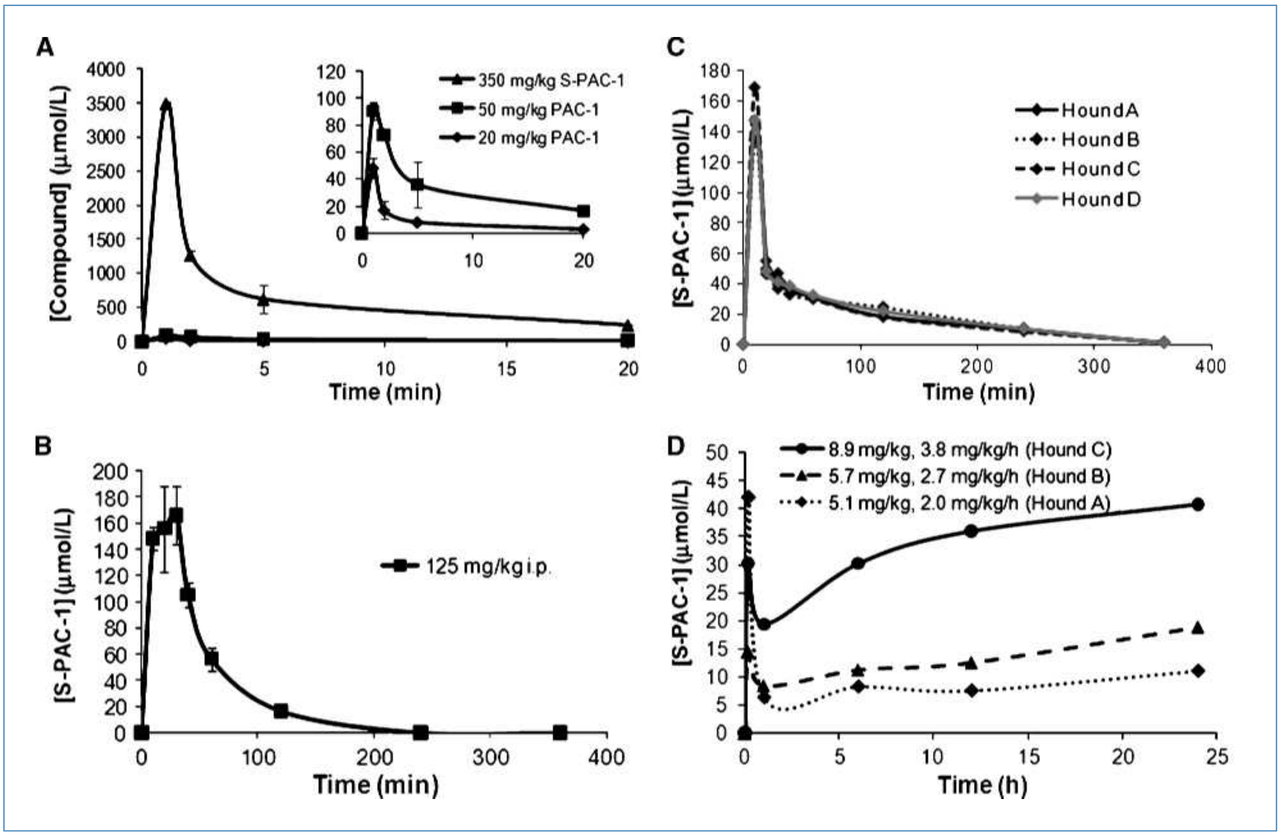

Figure 2. Serum concentrations of PAC-1 in mice and S-PAC-1 in mice and dogs. A, C57/BL6 mice were treated with 20 or 50 mg/kg PAC-1 or 350 mg/kg S-PAC-1 via tail vein injection. Mice were sacrificed at the times indicated, blood was drawn, and the concentration of drug was determined by HPLC. Points, mean (*n* = 2 for PAC-1 and *n* = 3 for S-PAC-1); bars, range for PAC-1; SE for S-PAC-1. B, serum concentration of S-PAC-1 after i.p. administration to mice. C57/BL6 mice were treated i.p. with 125 mg/kg S-PAC-1 and sacrificed at the times indicated, blood was drawn, and S-PAC-1 serum concentrations were determined by HPLC. Administration of 125 mg/kg S-PAC-1 provides a peak plasma concentration of ~170 μmol/L and a half-life of ~1 h. Points, mean (*n* = 3); bars, SE. C, four research hound dogs received a single i.v. dose of S-PAC-1 (25 mg/kg), blood was drawn at the time indicated, and S-PAC-1 serum concentration was determined by HPLC. D, three healthy hound dogs were each administered a different dose of S-PAC-1 by continuous i.v. infusion. Dogs received an initial loading dose (mg/kg, indicated in inset) over the course of 10 min followed by a constant-rate infusion (mg/kg/h) over the next 24 h. Blood was drawn at the times indicated, and the S-PAC-1 serum concentration was determined by HPLC. Continuous infusion of S-PAC-1 was well tolerated and successful in establishing a steady-state serum concentration of S-PAC-1 in dogs.

and 350 mg/kg S-PAC-1 (the highest dose tested) via tail vein injection. Serum was analyzed by high-performance liquid chromatography (HPLC) to provide the pharmacokinetic profiles for S-PAC-1 and PAC-1 (Fig. 2A). At the PAC-1 dosage that induced mild neurotoxicity (20 mg/kg), peak plasma concentrations were ~50 μmol/L. In contrast, a 350 mg/kg dose of S-PAC-1 provided peak plasma levels of ~3,500 μmol/L without any signs of neurotoxicity.

S-PAC-1 has a short half-life in mice

S-PAC-1 (125 mg/kg) was administered to mice via i.p. injection and found to have a short half-life (~1 hour, Fig. 2B); it was predicted that the mice would need to be treated with a 350 mg/kg dose of S-PAC-1 every 2 hours to achieve and maintain a minimum plasma concentration of 10 μmol/L over a course of 24 hours. Although this frequent dosing regimen for S-PAC-1 (i.p. every 2 hours for 24 hours) was technically feasible, further evaluation of S-PAC-1 as a novel therapeutic agent using murine tumor models was not methodologically practical. As such, we sought to further investigate S-PAC-1 in a larger mammalian experimental system, specifically healthy and spontaneous cancer-bearing dogs, which conferred greater practicality for the maintenance of S-PAC-1 steady-state concentrations for prolonged periods of time.

Assessment of S-PAC-1 in research dogs

Healthy research hound dogs were used for pharmacokinetic and toxicity investigations of S-PAC-1. First, four research hound dogs were treated with 25 mg/kg S-PAC-1 (solubilized in HPβCD) via i.v. injection over 10 minutes. In addition to pharmacokinetic analysis, the hematologic and nonhematologic tolerability of single-dose, i.v. S-PAC-1 administration was monitored in research dogs weekly for 4 consecutive weeks (Supplementary Table S2A). As shown in Fig. 2C, the peak plasma concentration resulting from this 25 mg/kg i.v. bolus dose was ~150 μmol/L. From analysis of the pharmacokinetic profile, the half-life of S-PAC-1 in dogs

Table 2. Noncompartmental pharmacokinetic analysis of S-PAC-1 (25 mg/kg) in four healthy research dogs

Parameters	Hound A	Hound B	Hound C	Hound D
Body weight (kg)	33.2	34.1	34.2	32.5
Lambda_z half-life (h)	1.05	1.11	1.11	1.09
T_{max} (h)	0.17	0.17	0.17	0.17
C_{max} (μg/mL)	69.86	63.71	80.07	69.83
$AUC_{0\text{-}inf}$ (h•μg/mL)	73.56	74.60	82.19	78.81
$AUMC_{0\text{-}inf}$ (h•h•μg/mL)	93.63	104.77	90.48	101.78
Cls (mL/h/kg)	340	335	304	317
Vss (mL/kg)	432.5	470.8	334.8	410
MRT (h)	1.27	1.40	1.10	1.29

Abbreviations: AUC, area under the curve; Cls, systemic clearance; Vss, volume of distribution at steady state; MRT, mean residence time.

was calculated to be 1.09 ± 0.02 hours (Table 2). Additionally, single-dose, i.v. S-PAC-1 treatment was well tolerated by all four research dogs, and no short- or long-term adverse events were observed with these animals as a result of treatment.

Based on the half-life of 1.09 ± 0.02 hours in dogs, continuous-rate infusion was explored in an attempt to maintain a steady-state serum concentration of S-PAC-1 during the course of the treatment. Three healthy research dogs were used to determine if S-PAC-1 could be safely administered via a continuous-rate infusion regimen, and to determine appropriate dosing levels to maintain plasma concentrations above ~10 μmol/L. Each dog received a different dose of S-PAC-1 (Fig. 2D) with an initial loading dose via i.v. infusion over the course of 10 minutes followed by a maintenance dose delivered by an infusion pump for an additional 24 hours. Each dog was observed throughout the course of the 24-hour infusions for adverse reactions, and blood was drawn at intervals to assess the pharmacokinetic profile of S-PAC-1 treatment. In addition, following completion of S-PAC-1 infusion, research dogs were evaluated for hematologic and nonhematologic toxicity weekly for 4 consecutive weeks. During this period, no dogs exhibited hematologic parameters outside of reference ranges (Supplementary Table S2B), and no adverse events were reported by animal care staff.

S-PAC-1 administered as a 24-hour continuous-rate infusion can be safely given to research dogs and easily reaches micromolar steady-state plasma concentrations that correlate with dose escalation (Fig. 2D). Based on these results, it was predicted that a 7 mg/kg loading dose and 3 mg/kg/h constant-rate infusion would be sufficient to achieve a steady-state plasma concentration of ~10 μmol/L.

Assessment of S-PAC-1 in dogs with lymphoma

Having confirmed the *in vitro* activity of S-PAC-1 and having shown that the compound can be safely administered via continuous-rate infusion and that steady-state plasma concentrations of S-PAC-1 of >10 μmol/L may be achieved for a 24-hour duration, a small (n = 6) clinical trial of client-owned pet dogs with spontaneous lymphoma was conducted. The aim of this trial was to show the feasibility of dosing S-PAC-1 in dogs with lymphoma and to determine if therapeutic serum levels of compound could be achieved via this dosing regimen. Pet dogs presented or referred to the Small Animal Clinic at the University of Illinois at Urbana-Champaign (UIUC) College of Veterinary Medicine were

Table 3. Characteristics of the six pet dogs with lymphoma treated with S-PAC-1

Patient	Breed	Male/female	Age	Weight (lb)	Immunophenotype	Prior therapy	Treatment (h)	Outcome
1	Mixed breed	Castrated male	7	79	B-cell lymphoma	CHOP	24	PR
2	Labrador Retriever	Spayed female	7	89	T-cell lymphoma	Naïve	24	SD
3	Newfoundland	Intact male	4	160	T-cell lymphoma	Naïve	24	SD
4	Welch Corgi	Spayed female	8	30	B-cell lymphoma	Naïve	72	SD
5	Golden Retriever	Spayed female	7	80	B-cell lymphoma	Naïve	72	PD
6	MC Boxer	Castrated male	6	59	T-cell lymphoma	Naïve	72	PD

Abbreviations: PD, progressive disease; PR, partial response; SD, stable disease.

considered for enrollment in the clinical trial (see Supplementary Data for inclusion criteria). Dogs that entered the study received treatment with S-PAC-1 as a single entity drug for 4 weeks and were followed for an additional 2 weeks after drug withdrawal.

Toxicity and pharmacokinetics of S-PAC-1 in canine lymphoma patients

Six patient dogs received treatment with S-PAC-1 via one of two treatment regimens (summarized in Table 3). Patients enrolled in the first treatment regimen (n = 3) received a once-a-week 24-hour continuous infusion of S-PAC-1 for four weekly cycles. Patients enrolled in the second treatment regimen (n = 3) received a 72-hour continuous infusion of S-PAC-1 every other week for two treatment cycles. Blood was collected during each S-PAC-1 treatment cycle for pharmacokinetic analysis. In addition, blood was collected from all pet dogs at each scheduled follow-up visit to characterize hematologic and nonhematologic toxicity. Between administrations, patients were monitored by pet owners for gastrointestinal toxicity observational scores adhering the VCOG-CTCAE (22). All patients enrolled in either treatment regimen did not show any clinically significant hematologic or nonhematologic toxicity (Supplementary Table S2C and D). Only minor adverse events were reported by pet owners, such as self-limiting and localized irritation at the infusion site (n = 4), transient loss of appetite (n = 1), and mild diarrhea (n = 3). All adverse reactions subsided within 48 hours of the end of each treatment cycle. Serum analysis indicated that all patients had measurable serum concentrations of S-PAC-1, as shown in Fig. 3. In accordance with our prediction from the healthy research dogs, an infusion with a loading dose of 7 mg/kg and a constant-rate infusion of 3 mg/kg/h was sufficient to achieve steady-state plasma concentrations of >10 μmol/L in the majority of treatments.

Antitumor activity of S-PAC-1

Given the small number of patients included in this clinical study, antitumor activity of S-PAC-1 cannot be conclusively determined. However, of the six patients treated, one patient (patient 1) showed a partial response with a ~30% reduction in both caliper RECIST score and the mandibular lymph node measurements by CT scan over the course of the 4-week treatment (Fig. 4A and B). During treatment, this dog received a 24-hour continuous i.v. infusion of S-PAC-1 once a

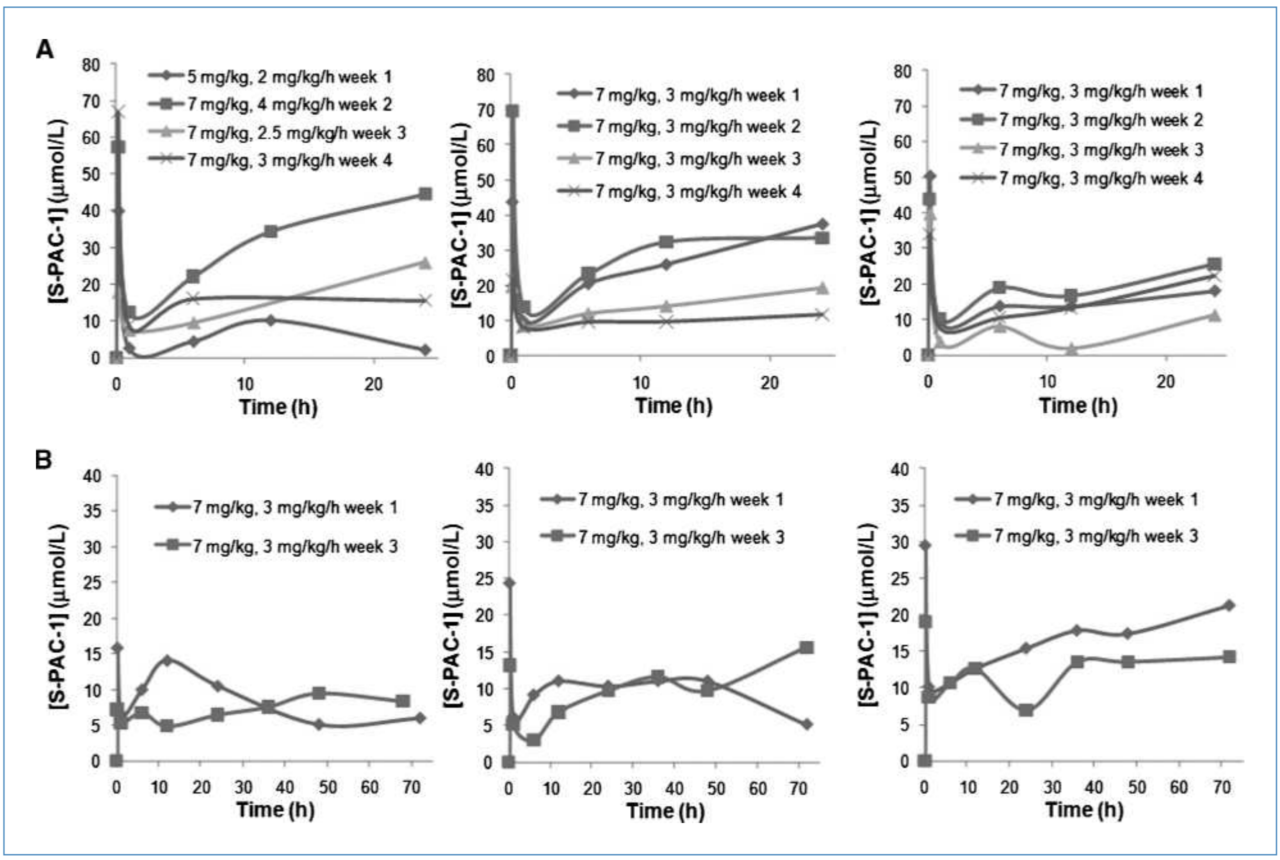

Figure 3. Serum concentrations of S-PAC-1 in six dogs with lymphoma enrolled in the clinical trial. Administration of S-PAC-1 as a constant-rate infusion was generally successful in achieving the target plasma concentration (10 μmol/L) for either 24 h (A, dogs 1–3) or 72 h (B, dogs 4–6). Data labels indicate doses (loading dose, mg/kg; continuous infusion dose, mg/kg/h) administered during the clinical trial. Blood was drawn at various times throughout drug administration, and serum concentration was determined by HPLC.

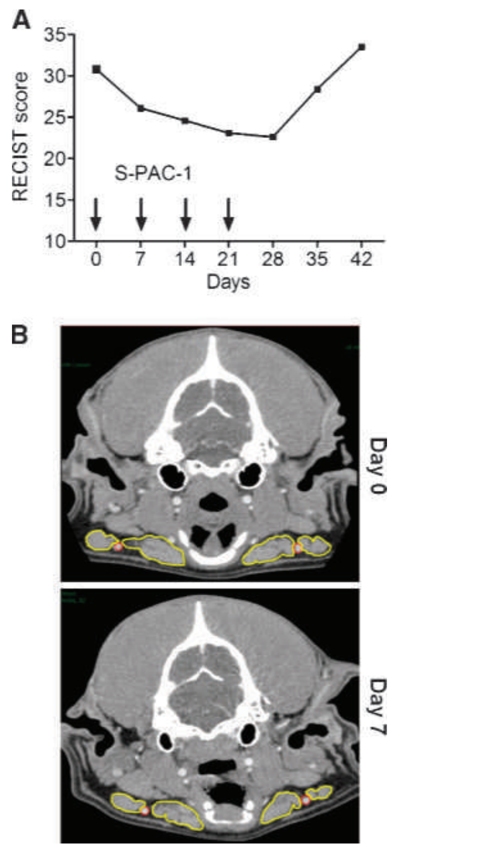

Figure 4. Activity of S-PAC-1 in patient 1. A, RECIST scores for patient 1 over the course of 7 wk. Arrows indicate days during which patient received S-PAC-1 as a 24-h continuous i.v. infusion (as detailed in text and Fig. 3A). After drug withdrawal, tumor size increased rapidly (days 28–42). B, CT scans of the mandibular lymph nodes of patient 1 (outlined in yellow) show a clinically measurable decrease in tumor size 1 wk after S-PAC-1 administration.

week (total of four treatments). Following the four treatment cycles, drug administration was withdrawn and the dog was monitored by RECIST for 2 subsequent weeks. After discontinuation of S-PAC-1 treatment, the RECIST scores for this dog increased dramatically (days 36 and 42). In addition to this partial response, three patients showed stable disease (patients 2–4), whereas two patients showed disease progression (patients 5 and 6), as indicated in Table 3. The rapid increase in RECIST scores after drug withdrawal shown in patient 1 is representative of the effect of drug withdrawal in all patients.

Analysis of lymph node aspirates from two dogs (patients 1 and 2) shows the presence of the procaspase-3 drug target before treatment as well as an increase in cleaved caspase-3 after treatment with S-PAC-1 (Supplementary Fig. S1). Lymph node aspirates collected from these dogs with lymphoma consisted of >90% malignant lymphocytes based on cytologic evaluation. Based on the predominance of malignant lymphocytes, the observed shift in cleaved caspase-3 after S-PAC-1 treatment (Supplementary Fig. S1) most likely represents the induction of apoptosis in malignant lymphocytes; however, a small percentage of this shift may be due to nonmalignant lymphocytes and stromal cells.

Discussion

S-PAC-1 is the first compound in the PAC-1 class (and the first small-molecule activator of procaspase-3) to be evaluated in a clinical trial of cancer patients. As such, the evaluation of S-PAC-1 in a clinical setting is a proof of concept for the strategy of direct procaspase-3 activation as an anticancer therapy. Compounds in the PAC-1 class activate procaspase-3 via chelation of inhibitory zinc ions (10). Intracellular zinc is found principally in tightly bound complexes in metalloproteinases, zinc finger domains, and other metal binding proteins; however, ~10% of cellular zinc is believed to exist in a loosely bound, labile pool (23). Several studies implicate labile zinc as an endogenous antiapoptotic regulator (24–26), and chelation of the loosely bound pool of zinc is an emerging anticancer strategy (9, 10, 27). Thus, the evaluation of S-PAC-1 is also a proof of concept for the chelation of the labile zinc pool as an anticancer therapy.

It is perhaps not surprising that high doses of PAC-1 induce neurotoxicity, given its zinc chelation properties and predicted BBB permeability. Zinc homeostasis is important in the CNS (28), and NMDA receptors require bound zinc to provide a tonic inhibition (17). NMDA receptors bind to zinc with a low affinity (K_d = 5.5 μmol/L; ref. 29), which suggests that a zinc chelator with a higher affinity for zinc such as PAC-1 (K_d = 52 nmol/L) would be able to successfully sequester zinc from these receptors. Several studies indicate that intracellular zinc chelation results in hyperexcitation of these receptors (16), resulting in symptoms such as uncontrolled muscle movement and seizure (17, 30). One strategy for reducing the permeability of a compound through the BBB is to increase the polarity of the molecule (18). Addition of the sulfonamide functional group is a good candidate for such polarity increase, as the aryl sulfonamide motif is common in several small-molecule therapeutics. The dramatically different neurotoxic effects of S-PAC-1 and PAC-1 suggest that S-PAC-1 is considerably less BBB permeable and may be the more attractive drug candidate.

Spontaneously arising cancers in pet dogs share many similarities with human cancers, including histologic appearance, tumor genetics, molecular targets, biological and clinical behavior, and response to therapy (31). Of these spontaneous canine cancers, multicentric lymphoma is the most common, occurring in 13 to 24 of every 100,000 dogs (32). The clinical progression and treatment of multicentric B- or T-cell canine lymphoma has many of the same characteristics of non–Hodgkin lymphoma in humans. Canine lymphoma and human non–Hodgkin lymphoma both respond clinically to the same cytotoxic drugs such as doxorubicin, vincristine, and cyclophosphamide. These drugs are components of the CHOP treatment protocol, first-line therapy for diffuse large B-cell lymphoma in humans (33). When administered to dogs, CHOP will induce complete clinical remission in ~90% of dogs diagnosed with lymphoma (34, 35). Similar to the human response, the majority of dogs who achieve remission with CHOP therapy will experience disease relapse (36). Given the commonalities between human and canine lymphoma, evaluation of S-PAC-1 in a canine lymphoma clinical trial may provide important translational information for the development of S-PAC-1 as a novel human therapeutic.

Although inconclusive in this study design, it is highly encouraging that four of six patients achieved partial response or stable disease for 4 weeks in duration, as canine lymphoma is generally a rapidly progressive malignancy with dramatic enlargement of peripheral lymph nodes within weeks of disease diagnosis. As shown in Table 3, one dog enrolled in the current study (patient 1) was in remission for 5 months after CHOP therapy and was recently diagnosed with recurrent lymphoma. On enrollment in the study, this dog showed a ~30% reduction in tumor size in response to S-PAC-1 treatment. This partial response is significant given the comparatively short treatment duration (4 weeks for S-PAC-1 versus 19 weeks for CHOP), and that the dose of S-PAC-1 administered does not seem to be near the maximum tolerated dose.

In conclusion, we have discovered S-PAC-1 as a procaspase-activating compound that can be safely administered *in vivo*, and have identified pet dogs with lymphoma as a tractable model for the assessment of small-molecule procaspase-3 activation as an anticancer strategy. The use of this large animal model allows drug administration via continuous-rate i.v. infusion, something necessary with S-PAC-1 (due to its short half-life *in vivo*) and not practical in murine tumor models. S-PAC-1 induces apoptotic death in cultured cancer cells, with similar activity to the parent compound PAC-1. Whereas high doses of PAC-1 (when administered in HPβCD) induce neurotoxicity *in vivo*, S-PAC-1 does not cause this effect at serum concentration ~70-fold higher. S-PAC-1 can be safely administered to mice, research dogs, and dogs with lymphoma and shows encouraging clinical effect in this preliminary evaluation. Given the absence of neurotoxicity with S-PAC-1 and the large safety window observed in mice, it is anticipated that S-PAC-1 will prove to be safe at escalated doses, and thus, its further evaluation in cancer patients is warranted.

Disclosure of Potential Conflicts of Interest

No potential conflicts of interest were disclosed.

Acknowledgments

We thank BioLine Rx for initial assistance with PAC-1 formulations.

Grant Support

NIH grant R01-CA120439 and UIUC. Q.P. Peterson was supported by NIH Chemistry-Biology Interface Training Grant NRSA 1-T32-GM070421 and by a predoctoral fellowship from the Medicinal Chemistry Division of the American Chemical Society. D.C. West was partially supported by National Research Service Award grant F31-CA130138-01S1.

The costs of publication of this article were defrayed in part by the payment of page charges. This article must therefore be hereby marked *advertisement* in accordance with 18 U.S.C. Section 1734 solely to indicate this fact.

Received 03/19/2010; revised 07/14/2010; accepted 07/19/2010; published OnlineFirst 09/07/2010.

References

1. O'Donovan N, Crown J, Stunell H, et al. Caspase 3 in breast cancer. Clin Cancer Res 2003;9:738–42.
2. Roy S, Bayly CI, Gareau Y, et al. Maintenance of caspase-3 proenzyme dormancy by an intrinsic “safety catch” regulatory tripeptide. Proc Natl Acad Sci U S A 2001;98:6132–7.
3. Krepela E, Prochazka J, Liul X, Fiala P, Kinkor Z. Increased expression of Apaf-1 and procaspase-3 and the functionality of intrinsic apoptosis apparatus in non-small cell lung carcinoma. Biol Chem 2004;385:153–68.
4. Izban KF, Wrone-Smith T, Hsi ED, Schnitzer B, Quevedo ME, Alkan S. Characterization of the interleukin-1b-converting enzyme/Ced-3-family protease, caspase-3/CPP32, in Hodgkin's disease. Am J Pathol 1999;154:1439–47.
5. Nakagawara A, Nakamura Y, Ikeda H, et al. High levels of expression and nuclear localization of interleukin-1 b converting enzyme (ICE) and CPP32 in favorable human neuroblastomas. Cancer Res 1997;57:4578–84.
6. Fink D, Schlagbauer-Wadl H, Selzer E, et al. Elevated procaspase levels in human melanoma. Melanoma Res 2001;11:385–93.
7. Persad R, Liu C, Wu T-T, et al. Overexpression of caspase-3 in hepatocellular carcinomas. Mod Pathol 2004;17:861–7.
8. Putt KS, Chen GW, Pearson JM, et al. Small-molecule activation of procaspase-3 to caspase-3 as a personalized anticancer strategy. Nat Chem Biol 2006;2:543–50.
9. Peterson QP, Goode DR, West DC, Ramsey KN, Lee J, Hergenrother PJ. PAC-1 activates procaspase-3 *in vitro* through relief of zinc-mediated inhibition. J Mol Biol 2009;388:144–58.
10. Peterson QP, Hsu DC, Goode DR, Novotny CJ, Totten RK, Hergenrother PJ. Procaspase-3 activation as an anti-cancer strategy: structure-activity relationship of PAC-1, and its cellular co-localization with procaspase-3. J Med Chem 2009;52:5721–31.
11. Paoloni M, Khanna C. Translation of new cancer treatments from pet dogs to humans. Nat Rev Cancer 2008;8:147–56.
12. Peterson QP, Goode DR, West DC, Botham RC, Hergenrother PJ. Preparation of the caspase-3/7 substrate Ac-DEVD-pNA by solution-phase peptide synthesis. Nat Protoc 2010;5:294–302.
13. Huang S, Clark RJ, Zhu L. Highly sensitive fluorescent probes for zinc ion based on triazolyl-containing tetradentate coordination motifs. Org Lett 2007;9:4999–5002.
14. Brewster ME, Simpkins JW, Hora MS, Stern WC, Bodor N. The potential use of cyclodextrins in parenteral formulations. J Parenter Sci Technol 1989;43:231–40.
15. Padhani AR, Ollivier L. The RECIST (Response Evaluation Criteria in Solid Tumors) criteria: implications for diagnostic radiologists. Br J Radiol 2001;74:983–6.
16. María-Isabel D, José-Miguel B-I, Carlos C, Juan N, Ana-Isabel M-M, Francisco-José M-G. Neural overexcitation and implication of NMDA and AMPA receptors in a mouse model of temporal lobe epilepsy implying zinc chelation. Epilepsia 2006;47:887–99.
17. Domínguez MI, Blasco-Ibez JM, Crespo C, Marqus-Mar AI, Martnez-Guijarro FJ. Zinc chelation during non-lesioning overexcitation results in neuronal death in the mouse hippocampus. Neuroscience 2003;116:791–806.
18. Clark DE. *In silico* prediction of blood-brain barrier permeation. Drug Discov Today 2003;8:927–33.
19. Lavoie N, Peralta MR III, Chiasson M, et al. Extracellular chelation of zinc does not affect hippocampal excitability and seizure-induced cell death in rats. J Physiol 2007;578:275–89.

20. Bose K, Pop C, Feeney B, Clark AC. An uncleavable procaspase-3 mutant has a lower catalytic efficiency but an active site similar to that of mature caspase-3. Biochemistry 2003;42:12298–310.
21. Vichai V, Kirtikara K. Sulforhodamine B colorimetric assay for cytotoxicity screening. Nat Protoc 2006;1:1112–6.
22. Veterinary Co-operative Oncology Group—Common Terminology Criteria for Adverse Events (VCOG-CTCAE) following chemotherapy or biological antineoplastic therapy in dogs and cats v1.0. Vet Comp Oncol 2004;2:195–213.
23. Franklin RB, Milon B, Feng P, Costello LC. Zinc and zinc transporters in normal prostate and the pathogenesis of prostate cancer. Front Biosci 2005;10:2230–9.
24. Aiuchi T, Mihara S, Nakaya M, Masuda Y, Nakajo S, Nakaya K. Zinc ions prevent processing of caspase-3 during apoptosis induced by geranylgeraniol in HL-60 cells. J Biochem (Tokyo) 1998;124:300–3.
25. Chai F, Truong-Tran AQ, Ho LH, Zalewski PD. Regulation of caspase activation and apoptosis by cellular zinc fluxes and zinc deprivation: a review. Immunol Cell Biol 1999;77:272–8.
26. Chimienti F, Seve M, Richard S, Mathieu J, Favier A. Role of cellular zinc in programmed cell death: temporal relationship between zinc depletion, activation of caspases, and cleavage of Sp family transcription factors. Biochem Pharmacol 2001;62:51–62.
27. Huesca M, Lock LS, Khine AA, et al. A novel small molecule with potent anticancer activity inhibits cell growth by modulating intracellular labile zinc homeostasis. Mol Cancer Ther 2009;8:2586–96.
28. Frederickson CJ, Koh J-Y, Bush AI. The neurobiology of zinc in health and disease. Nat Rev Neurosci 2005;6:449–62.
29. Karakas E, Simorowski N, Furukawa H. Structure of the zinc-bound amino-terminal domain of the NMDA receptor NR2B subunit. EMBO J 2009;28:3910–20.
30. Adler M, Dinterman RE, Wannemacher RW. Protection by the heavy metal chelator *N,N,N′,N′*-tetrakis (2-pyridylmethyl)ethylenediamine (TPEN) against the lethal action of botulinum neurotoxin A and B. Toxicon 1997;35:1089–100.
31. Breen M, Modiano JF. Evolutionarily conserved cytogenetic changes in hematological malignancies of dogs and humans—man and his best friend share more than companionship. Chromosome Res 2008;16:145–54.
32. Dorn CR, Taylor DO, Schneider R. The epidemiology of canine leukemia and lymphoma. Bibl Haematol 1970;36:403–15.
33. Kahl B. Chemotherapy combinations with monoclonal antibodies in non-Hodgkin's lymphoma. Semin Hematol 2008;45:90–4.
34. Garrett LD, Thamm DH, Chun R, Dudley R, Vail DM. Evaluation of a 6-month chemotherapy protocol with no maintenance therapy for dogs with lymphoma. J Vet Intern Med 2002;16:704–9.
35. Chun R, Garrett LD, Vail DM. Evaluation of a high-dose chemotherapy protocol with no maintenance therapy for dogs with lymphoma. J Vet Intern Med 2000;14:120–4.
36. Rassnick KM, Mauldin GE, Al-Sarraf R, Mauldin GN, Moore AS, Mooney SC. MOPP chemotherapy for treatment of resistant lymphoma in dogs: a retrospective study of 117 cases (1989-2000). J Vet Intern Med 2002;16:576–80.